

Four-wave resonance in electrohydrodynamic convection

Manuel de la Torre Juárez and Ingo Rehberg

Physikalisches Institut der Universität Bayreuth, 8580 Bayreuth, West Germany

(Received 7 March 1990)

The supercritical Hopf bifurcation to oblique traveling rolls in nematic liquid crystals leads to a complex spatiotemporal state. We present an experimental study of the bifurcation scenario in which a secondary bifurcation to a coherent steady state occurs at higher values of the control parameter. Temporal resonant modulation of the driving force can stabilize the four amplitude modes appearing after the first bifurcation, and their superposition can lead to a standing bimodal pattern.

I. INTRODUCTION

Electrohydrodynamic convection of nematic liquid crystals¹ (EHC) provides a convenient system to study pattern-formation processes in an anisotropic system. It offers the experimental advantages of having easily controllable external parameters together with short time scales even in large cells containing hundreds of rolls. The experimental evidence of a direct bifurcation to traveling waves² (TW) makes EHC an appropriate experimental system to study the influence of a resonant time modulation of the driving force on the TW. It has been shown, theoretically³ and experimentally,⁴ that by modulating the external control parameter R (i.e., the ac-voltage amplitude) in the form $R(t) = R_c [1 + \epsilon + b \cos(\omega_m t)]$ with a modulation frequency ω_m of about twice the Hopf frequency, standing waves (SW) can be stabilized by an appropriate choice of the modulation amplitude b and the reduced voltage amplitude $\epsilon = R/R_c - 1$.

The available theory³ was developed for a system with only one spatial dimension in which two amplitude modes exist: one corresponding to the left TW, and a second for the right TW. This theory can be applied in EHC, provided that the rolls are perpendicular to the initial orientation of the director. However, it is well known for EHC that it is also possible to have rolls with an oblique orientation.^{5,6} Each, the left and the right traveling amplitude modes, then splits into two oblique amplitude modes corresponding to the two possible signs of the orientation of the angle. The theory must then be extended to a two-dimensional model in space that describes this four-mode interaction. Similar interactions are known in the context of surface gravity waves,^{7,8} or in the transition from axisymmetric Taylor vortices to wavy vortex flow.⁷ This report deals with the experimental results concerning the four-wave resonance appearing when a supercritical Hopf bifurcation is present in the EHC oblique-roll regime.

The experimental setup and procedure are described in Ref. 9. The samples studied are about 13 μm thick. The region observed included 30–60 wavelengths in both directions x (parallel to the director) and y (perpendicular to the director). Inhomogeneities of the cell (either due

to geometrical or chemical ramps) produce a threshold shift that has been measured to be less than 0.1% in the x direction and about 0.3% in the y direction.

The cells were filled with the nematic liquid crystal, Merck Phase V: a mixture of azoxy compounds with a small negative dielectric anisotropy of $\epsilon_a \equiv \epsilon_{\parallel} - \epsilon_{\perp} = -0.2$, which favors the creation of oblique rolls. The electrodes are rubbed in one direction to impose an initial homogeneous planar orientation of the director field. The cells are kept inside a thermalized box to achieve a temperature stabilization of about ± 0.003 K and are hermetically sealed in order to avoid impurities coming from the outside into the fluid. This produces a good stability of the values of the bifurcation diagrams for weeks.

A modulated ac voltage produced by a synthesizer is applied to the transparent electrodes. The voltage has the form $V(t) = V_c \cos(\omega t) [1 + \epsilon + b \cos(\omega_m t)]$, with V_c being the threshold voltage at the driving frequency $f = \omega/2\pi$ without modulation [$\epsilon = (V - V_c)/V_c$], and b and $f_m = \omega_m/2\pi$ are the amplitude and the frequency of the modulation, respectively.

The measurements were done by means of a shadow-graph technique.¹⁰ A collimated beam of light polarized parallel to the orientation of the director field traverses the cell along the direction of the electric field. The resulting image is acquired with a charge-coupled device (CCD) camera mounted to a microscope and digitized (512 \times 512 pixel, 256 gray levels). The digitized images are stored and processed on a microcomputer.

II. TRAVELING OBLIQUE ROLLS

It is well known that at frequencies below the so-called Lifschitz point,⁵ Williams rolls appear with an orientation oblique to the director field. We investigate the onset of these rolls by measuring the intensity modulation of the transmitted light along a line parallel to the director field. A value for the distortion of the director field is obtained by calculating the standard deviation of this line from the undistorted line. This procedure gives a measure of the contrast of the image, which has been shown¹⁰ to be proportional to the director angle θ , i.e., the amplitude of convection. A close investigation of the onset of oblique rolls in our thin cells shows three different re-

gimes when increasing the voltage (see Fig. 1).

(i) Between 5.3 and 5.385 eV (see inset in Fig. 1), the contrast increases. This is caused by small incoherent bursts of the light intensity. Presumably, this is an amplification of the fluctuations of the director around its equilibrium position, which becomes more effective close to the convection threshold. The typical wavelength of the convection rolls is not observable in this state.

(ii) Above 5.3850 V, the state changes its character. Now the roll structure becomes apparent, although the rolls are almost invisible to the eye. This low-amplitude state shows no coherent spatial pattern, but an irregular dynamic cellular structure. It can best be described as a superposition of randomly positioned patches of left and right oblique TW [see Figs. 2(a) and 3].

(iii) When increasing the voltage amplitude continuously, there is a sudden transition at 5.4400 V to a stable steady pattern [Fig. 2(b)] with a much higher convection amplitude. Because the low-amplitude traveling state (ii) was not observed in Ref. 9, this steady regime was incorrectly assumed to come via a primary bifurcation from the ground state. The height of the amplitude jump shown here can be estimated to be at least ten times the value of the low amplitude. In order to observe region (ii) clearly, the focal plane of the microscope was chosen very high above the cell; therefore the measurement method saturates very soon in regime (iii) and keeps the contrast almost constant above a given value of the voltage in Fig. 1.

The hysteresis measured in this transition is 0.01 ± 0.0025 V. When decreasing the voltage, the pattern starts to decay in the neighborhood of grain boundaries or the lateral boundaries, where the amplitude is close to zero. Presumably, in the absence of these imperfections, the hysteresis would be larger.

The onset of the low-amplitude convection [state (ii)] is frequency dependent, as shown in Fig. 4(b). The solid circles indicate the onset of the conductive rolls, while the open circles correspond to the onset of the dielectric rolls.¹ The range of the low-amplitude TW state is then shown in Fig. 4(a). It is small for low frequencies and in-

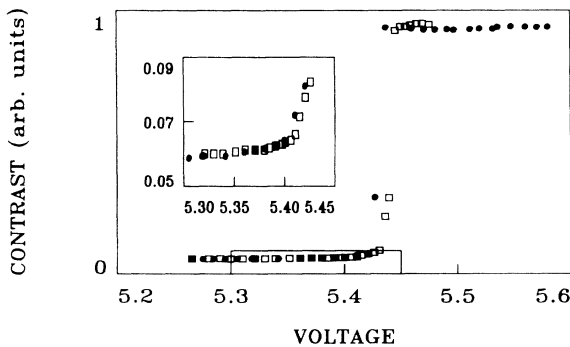


FIG. 1. Root mean square of the light intensity on a line along the initial orientation of the director vs effective voltage. In the small inset, the first bifurcation can be seen in detail. Open squares have been measured by slowly increasing the voltage and solid circles correspond to the inverse process.

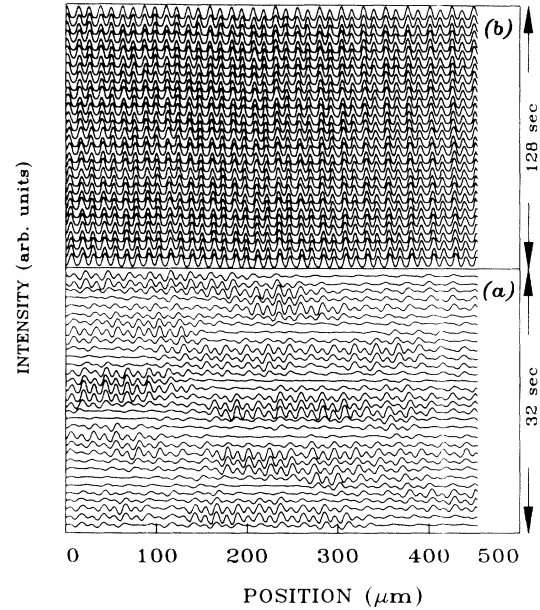


FIG. 2. Intensity lines plotted above each other as a function of time for constant voltages. The intensities are normalized to obtain a clear picture in the low-amplitude state. (a) Oscillatory state, $\epsilon = 0.009$; (b) steady state, $\epsilon = 0.019$, at a driving frequency of $0.031f_c$.

creases drastically at higher frequencies. In order to show that this phenomenon is very robust, curves for different temperatures have been measured and are shown in Fig. 4(a). When the frequency is rescaled with respect to the critical frequency f_c , at which dielectric rolls first appear, the curves are similar. Above the reduced frequency of 0.65, the transition to state (iii) is replaced by the onset of defects; thus no steady state can be seen.

At the onset of the steady state (iii), the angle of the oblique rolls is frequency dependent, as shown in Fig.

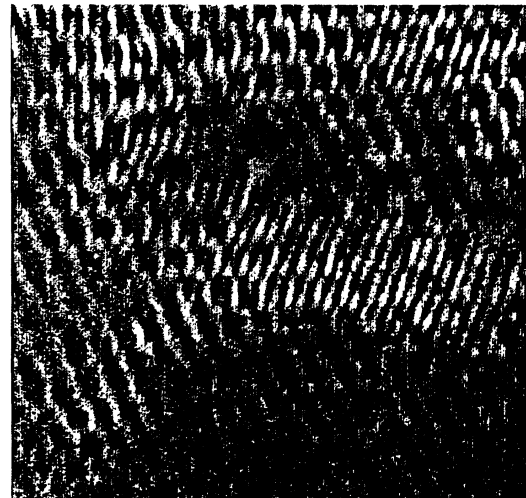


FIG. 3. Spatial structure at the traveling oblique regime.

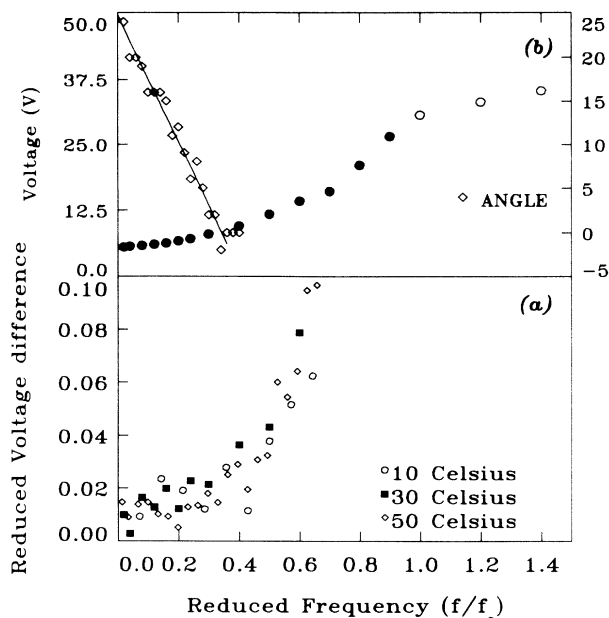


FIG. 4. (b) Convection threshold as a function of the reduced frequency for the conductive regime (●) and for the dielectric regime (○) at $T=30^\circ\text{C}$. Open diamonds indicate the angle of obliqueness α at the onset of steady convection in degrees, indicated on the right-hand-side scale. The solid line, $\alpha=24.74-72.43f$, is obtained from a linear fit. (a) The range of oblique TW for three different temperatures.

4(b). This angle seems to approach zero following a linear dependence. For a linear state, the angle should decay as a square-root function of f/f_c , but this is not necessarily the case for a nonlinear state. This measurement is similar to the unexpected angle versus frequency behavior described in Ref. 9. After checking the cell used for that measurement, state (ii) was also observed in that cell.

The angle at the onset of state (ii) could not be measured precisely because of the instability of this structure; but the fact that it decreases with increasing frequency is clearly visible. Above the critical frequency $f_L=0.34$, where the angle becomes zero, the state (ii) consists of incoherent normal TW. Because their spatial correlation increases both with increasing ϵ and increasing frequency, it is possible to observe extended regions of coherent TW at higher frequencies, similar to the ones described in Ref. 4.

III. MODULATED TRAVELING OBLIQUE ROLLS

When modulating the driving force on a one-dimensional system showing a Hopf bifurcation, a resonant behavior can be observed at a modulation frequency of about double the Hopf frequency.^{3,11} The modulation of the traveling oblique rolls also shows a resonant response: In Fig. 5 one can see that for a reduced driving frequency ($f=0.031f_c$), a subcritical reduced voltage ($\epsilon=-0.05$), and a constant modulation amplitude ($b=10\%$), only by changing the modulation frequency

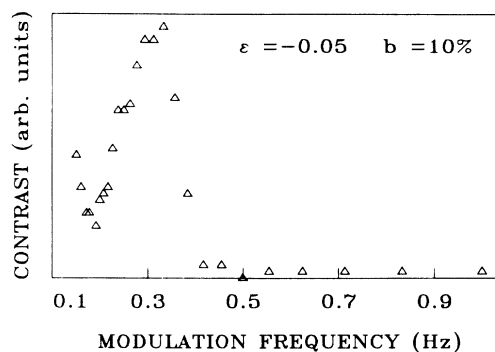


FIG. 5. Contrast of the transmitted light measured along a line as a function of the modulation frequency for $f=0.031f_c$. The resonance peak is at $f_m=0.313$ Hz.

can one get a transition from the ground state (above 0.4 Hz) to convection. The resonance peak is at 0.313 Hz, which is approximately double the frequency of the TW shown in Fig. 2(a). On the left of this maximum, the structure appears again. Here it becomes difficult to observe a resonance phenomenon, however, because the structure follows adiabatically the slow modulation of ϵ from subcritical to supercritical values at these low frequencies. Figure 5 supports the idea that a Hopf bifurcation is responsible for the oblique TW.

Resonant modulation is known to couple the left and the right TW amplitude modes to get a SW in the one-dimensional case.^{3,4} In the case of oblique TW [state (ii)], one deals with four modes that correspond to the two directions of inclination each traveling to the left and to the right. If all four modes are stabilized with the same amplitude, their superposition gives a standing bimodal solution. In the experiment, the four-mode coupling leads to spatiotemporal incoherent behavior (ii), but a regular structure can be obtained by means of a resonant temporal modulation of the driving force (Fig. 6).

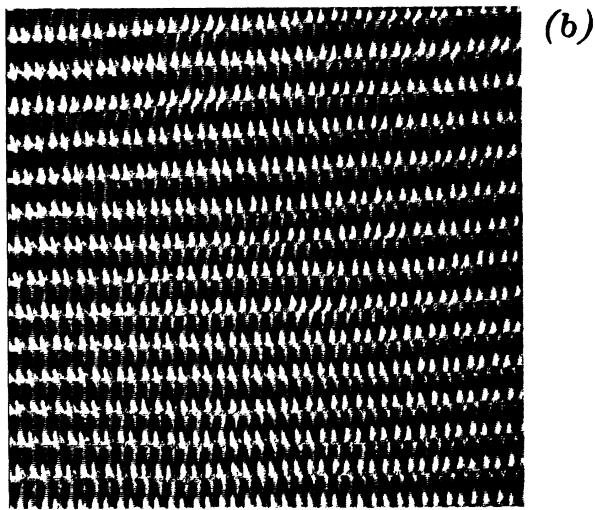
The perfect standing bimodal pattern, shown in Fig. 6(b), could be stabilized for hours over all the sample at $0.0296f_c$. The coupling is dependent on the driving frequency—at $0.111f_c$, the structure is a standing oblique pattern with a small spatially periodic modulation [Fig. 6(a)]. The transition from one state to the other seems continuous: Above $0.031f_c$, the bimodal pattern starts showing imperfections in the form of localized small areas of slightly modulated oblique rolls. The extension of these oblique regions increases with the driving frequency (as the angle decreases) until $0.148f_c$, where the spatial modulation of the rolls vanishes and gives way to a standing oblique structure.

The influence of ϵ and b on the behavior of the system is summarized in Fig. 7. The open circles indicate the onset of convection, i.e., state (ii). For low-modulation amplitudes, one has a similar scenario as in the case without modulation; but now the TW appear modulated in amplitude and frequency. At larger ϵ , there is the sudden transition to the high-amplitude steady mode (iii) indicated by the solid squares.

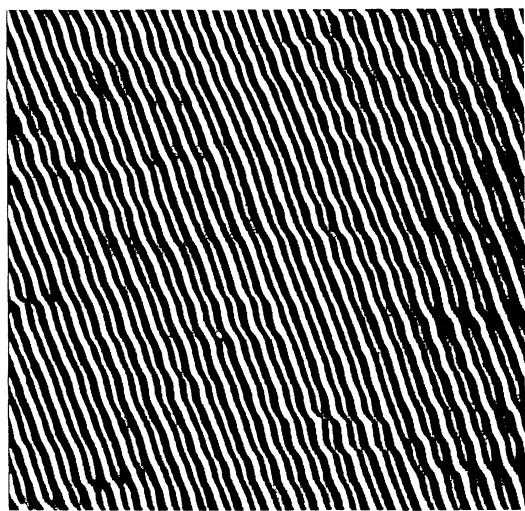
When increasing the modulation amplitude, the

patches of TW are replaced by patches of SW, as shown in Fig. 8(a). Because of the irregular behavior of both states, the transition from one to another is difficult to pinpoint. In Fig. 7(a) there is a decrease of the threshold voltage above modulation amplitudes of 3%, which is very reminiscent of the behavior observed for normal rolls.³ The transition from traveling to standing patches seems to take place here.

At a higher modulation amplitude, the scenario is more complex. Figure 8 summarizes the different states observed at a modulation amplitude of 10%, at a modulation frequency of 0.5 Hz. Between $\epsilon = -0.051$ and -0.012 , patches of SW are observed [Fig. 8(a)]. The spa-



(b)



(a)

FIG. 6. Bimodal patterns of SW at a driving frequency of (a) $0.111f_c$ and (b) $0.0296f_c$.

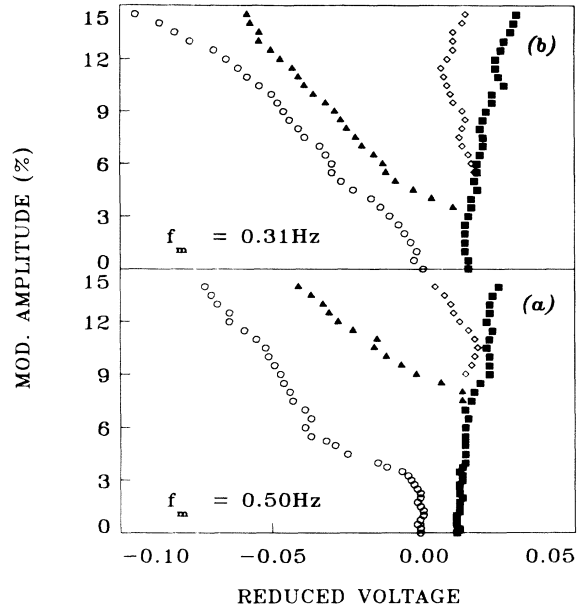


FIG. 7. Phase diagram at $f = 0.031f_c$ for a modulation frequency of (a) $f_m = 0.5$ Hz and (b) $f_m = 0.31$ Hz. Open circles indicate the onset of low-amplitude convection; solid triangles give the onset of the stable standing convective structures; the open-diamond line is the threshold of chaotic behavior; the squares correspond to the onset of a modulated steady structure.

tial structure is similar to that shown in Fig. 3. At $\epsilon = -0.012$, a sudden jump in the amplitude (about a factor of 5) can be observed (solid triangles in Fig. 7). Above this transition, a stable standing bimodal structure [Fig. 8(b)] similar to the one shown in Fig. 5 exists.

At higher ϵ values (open diamonds) this state loses sta-

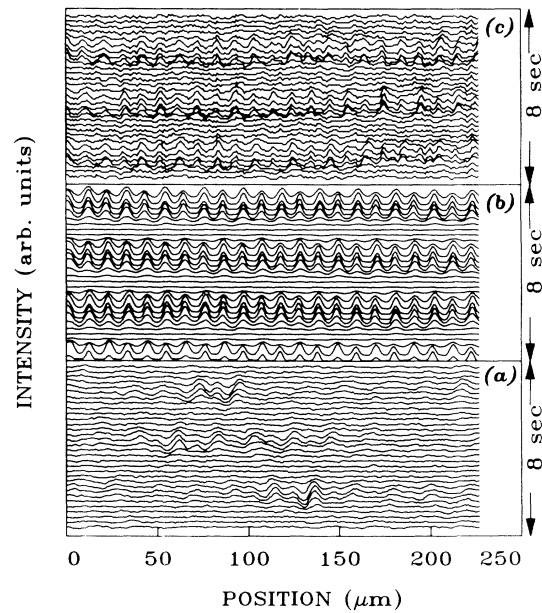


FIG. 8. Time evolution of the normalized intensity lines for three different solutions at $f = 0.031f_c$, $b = 10\%$, and $f_m = 0.5$ Hz: (a) Patches of SW at $\epsilon = -0.02$; (b) bimodal SW at $\epsilon = 0$; (c) chaotic state at $\epsilon = 0.02$.

bility and shows complicated dynamical behavior [Fig. 8(c)]: It appears as an oblique pattern alternating in time between both directions ("zig" and "zag") of inclination. Within one period, when the convection amplitude increases, the pattern might appear as a "zig" mode. During the peak of the amplitude, the pattern appears bimodal; during the decay, the "zag" mode will dominate. This behavior has no strong spatial coherence.

At higher ϵ values (solid squares), one gets a steady oblique-roll structure that is temporally modulated in amplitude with the modulation frequency. At other modulation frequencies [Fig. 7(b)], the scenario is similar. Here the modulation frequency of $f_m = 0.31$ Hz is closer to the resonance peak, which might explain that the transition to the bimodals (solid triangles) appears at a lower modulation amplitude of 3.5%.

IV. SUMMARY AND CONCLUSIONS

It has been shown that steady oblique rolls can appear in thin cells as a secondary instability. This may explain our failure in observing a square-root law for the angle of oblique rolls as a function of the frequency, as would be expected when the oblique rolls stem from a primary bifurcation. In our earlier investigations, states corresponding to (i) and (ii) were not observed. This is explained by the fact that the amplitude of these states is very small. Once we became aware of them, we found similar states in all the thin cells we have checked since then, both in Phase V and the standard nematic liquid-crystal methoxybenzylidene butylaniline (MBBA). In cells with a thickness larger than $50 \mu\text{m}$, these states were not observed. Whether this is simply due to the reduced sensitivity of the shadowgraph method, or whether the effect itself vanishes, is currently unclear.

The existence of the low-amplitude TW state also sheds some light on the nature of the oscillatory instability. At low frequencies, the range of the oscillatory behavior is

very small; the situation is reminiscent of double diffusive convection, where the manifestation of binary mixture effects can also be observed in a small ϵ range only. At higher frequencies, the transition from state (ii) to state (iii) vanishes, and the amplitude and spatial coherence of the TW state increases smoothly with ϵ . Thus in this range it is more obvious experimentally that the first bifurcation is an oscillatory one. In addition, obviously, the spatial coherence of the structure at a fixed ϵ increases with increasing frequency. This might have to do with the fact that the angle of obliqueness influences the stability of the interaction of the four modes.

Most importantly, it has been shown that oblique TW appear as a very low-amplitude mode at threshold. Their interaction leads to incoherent structures, but by resonant modulation the modes can be stabilized to form a bimodal structure. The spatial homogeneity of the bimodal structure is frequency dependent; again, this can be due to the change of the angle of obliqueness of the modes. This observation is coherent with the fact that theoretical calculations made without modulation show that the angle of the oblique rolls increases as one gets closer to the transition to bimodals; and for decreasing angle of obliqueness, one always expects oblique rolls to become favorable. For large angles, bimodals start to become apparent in the neighborhood of grain boundaries, although they have been observed to be always unstable against oblique rolls.¹² Because the amplitudes of these states are small, an explanation via amplitude equations for the four coupled modes seems possible.

ACKNOWLEDGMENTS

We wish to thank W. Zimmermann, L. Kramer, S. Rasenat, and F. H. Busse for very useful suggestions and comments. One of us (M.T.J.) thanks the Spanish Ministerio de Educación y Ciencia for financial support. The experiments were supported by the Forschungsgemeinschaft.

¹P. G. de Gennes, *The Physics of Liquid Crystals* (Clarendon, Oxford, 1974); E. Bodenschatz, W. Zimmermann, and L. Kramer, *J. Phys. (Paris)* **49**, 1875 (1988).

²S. Kai and K. Hirakawa, *Mol. Cryst. Liq. Cryst.* **40**, 261 (1977); A. Joets and R. Ribotta, *Phys. Rev. Lett.* **60**, 2164 (1988); I. Rehberg, S. Rasenat, and V. Steinberg, *ibid.* **62**, 756 (1989).

³H. Riecke, J. D. Crawford, and E. Knobloch, *Phys. Rev. Lett.* **61**, 1942 (1988); D. Walgraef, *Europhys. Lett.* **7**, 485 (1988).

⁴I. Rehberg, S. Rasenat, J. Fineberg, M. de la Torre Juárez, and V. Steinberg, *Phys. Rev. Lett.* **61**, 2449 (1988).

⁵W. Zimmermann and L. Kramer, *Phys. Rev. Lett.* **55**, 402 (1985); R. Ribotta, A. Joets, and Lin Lei, *ibid.* **56**, 1595 (1986).

⁶W. Pesch and L. Kramer, *Z. Phys. B* **63**, 121 (1986).

⁷A. Craik, *Wave Interactions and Fluid Flows* (Cambridge University Press, Cambridge, 1985).

⁸M. Silber, Ph.D. thesis, University of California, Berkeley, 1989 (unpublished).

⁹I. Rehberg, B. L. Winkler, M. de la Torre Juárez, and W. Schöpf, in *Festkörperprobleme/Advances in Solid-State Physics*, edited by U. Rössler (Vieweg, Braunschweig, 1989), Vol. 29, p. 35.

¹⁰S. Rasenat, B. L. Winkler, G. Hartung, and I. Rehberg, *Exp. Fluids* **7**, 412 (1989).

¹¹M. de la Torre Juárez and I. Rehberg, in *New Trends in Non-linear Dynamics and Pattern Forming Phenomena: The Geometry of Nonequilibrium*, NATO Advanced Study Institute, edited by P. Coulet and P. Huerre (Plenum, New York, in press).

¹²L. Kramer, E. Bodenschatz, W. Pesch, W. Thom, and W. Zimmermann, *Mol. Cryst. Liq. Cryst.* **5**, 699 (1989).

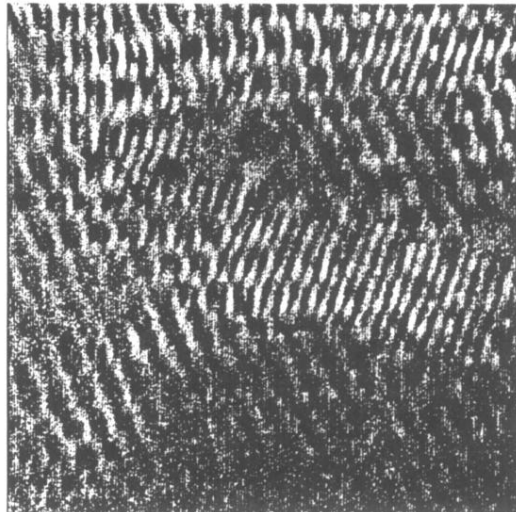


FIG. 3. Spatial structure at the traveling oblique regime.

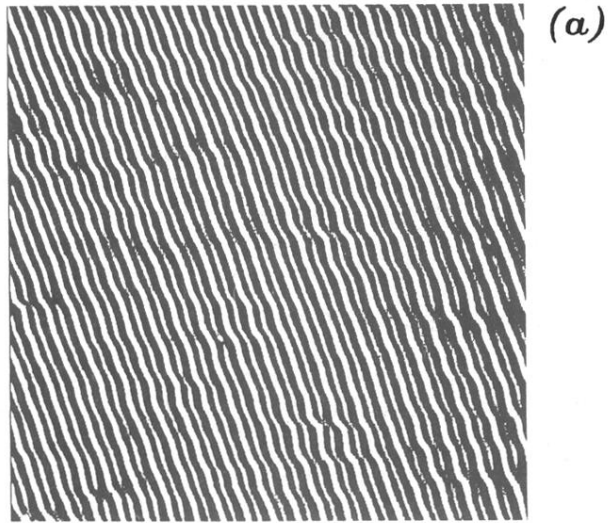
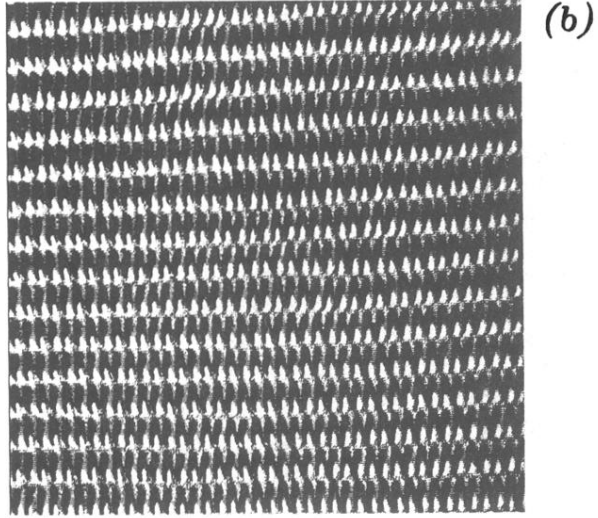


FIG. 6. Bimodal patterns of SW at a driving frequency of (a) $0.111f_c$ and (b) $0.0296f_c$.